

Measurement of (n, f) and (n, xn) cross sections with surrogate reaction method

Nanru Ma¹, Chengjian Lin^{1,*}, Huiming Jia¹, Xinxing Xu¹, Feng Yang¹, Lei Yang¹, Lijie Sun¹, Dongxi Wang¹, Huanqiao Zhang¹, and Zuhua Liu^{1,**}

¹China Institute of Atomic Energy, P.O. Box 275(10), Beijing 102413, China

Abstract. Surrogate reaction method is an important approach to overcome the difficulties meet in the direct measurement of neutron induced nuclear reaction. The current existing surrogate reactions generally employ the peripheral reactions such as inelastic excitation and transfer reaction where the involved angular momenta are much larger than the neutron capture reaction, which causes a difficulty in theoretical correction of spin of compound nucleus. We proposed to use capture reaction of light charged particle as the surrogate reaction, thus the spin distributions of compound nucleus in two reactions are quite similar and therefore the spin correction is not strongly desired. Based on this idea, the $^{239}\text{Pu}(n, f)$ and $(n, 2n)$ cross sections were successfully extracted by using $^{236}\text{U}(\alpha, f)$ and $(\alpha, 2n)$ reactions as the surrogate reactions. The well coincidence of the present results with the data of ENDFB7 within the error bars shows the reliability of the proposed surrogate capture reaction method.

1 Introduction

Nuclear power today makes a significant contribution to electricity generation, providing about 10% of global electricity supply. The design of advanced nuclear reactors for power supply and nuclear waste transmutation calls for some key nuclear data urgently, especially the neutron induced reaction data. However, due to the limited energies for the neutron beams, the short-lived target nuclides and strong radioactivity, many neutron induced reaction data are very difficult to measure directly. Especially for $(n, 2n)$ reaction which plays an essential role in nuclear waste transmutation, the direct measurement is even harder due to the interference caused by the background neutrons from scattering and fission, etc. The surrogate reaction method (SRM) overcomes the difficulties meet in the direct measurement for the neutron induced reaction cross sections effectively.

1.1 surrogate reaction method

SRM refers to an indirect method which uses an surrogate reaction with a more experimentally accessible or preferable combination of projectile "d" and target "D" in measuring the target neutron "a" induced reaction cross sections, as shown in Figure 1 [1]. The basic principle is that the same compound nucleus (CN) "B" with the same excitation energy (E_x) can be formed by selecting a suitable reaction channel, based on the idea for the equilibrated compound nucleus that the formation phase is independent of the decay phase (if omitting the small difference for the angular momentum).

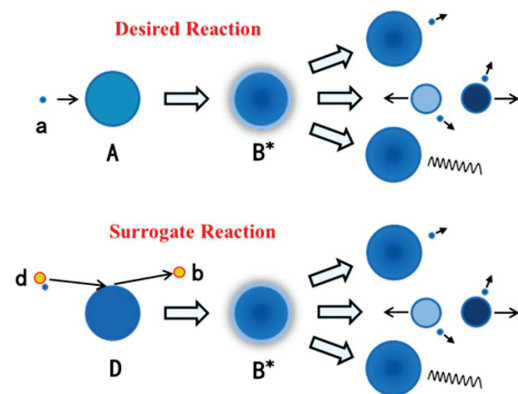


Figure 1. Schematic diagram of SRM.

SRM was proposed in the early 1970s by Cramer J D and Britt H C, who used (t, pf) two-neutron transfer reaction as the surrogate reaction in the measurement of the (n, f) cross sections of the actinide nuclei [2]. For example, $^{230,232}\text{Th}$, $^{234,236,238}\text{U}$ and $^{240,242}\text{Pu}(t, pf)$ were used as the surrogate reactions for $^{231,233}\text{Th}$, $^{235,237,239}\text{U}$ and $^{241,243}\text{Pu}(n, f)$ respectively, through a simple formula:

$$\sigma_{nf}(E_n) = \sigma_C(E_n)P_{(t,pf)}^{exp}(E_n), \quad (1)$$

$\sigma_{nf}(E_n)$ and $\sigma_C(E_n)$ are respectively the neutron induced fission cross section and the neutron capture cross section at the energy E_n , and $P_{(t,pf)}^{exp}(E_n)$ is the experimental measured fission probability of the surrogate reaction at the corresponding neutron energy E_n ,

$$P_{(t,pf)}^{exp}(E_n) = N_f/N_p, \quad (2)$$

*Corresponding author, e-mail: cjlin@ciae.ac.cn
 **Deceased

N_p and N_f are the proton counts from transfer reaction and the fission counts, respectively. After decades of development, especially the blowout type development after 2000 [3][4], now SRM has different forms like surrogate ratio method [3], surrogate capture reaction method and so on.

1.2 Surrogate Ratio Method

Surrogate ratio method obtains the reaction cross section by measuring the ratio of the cross section of the desired reaction channel to that of a well-measured reaction channel, which means that the higher data accuracy the selected reference reaction channel has, the better data the target reaction channel can be obtained.

According to the difference of the reference reaction channels, surrogate ratio method can be divided into the two types of internal ratio method [3] and external ratio method [4]. The internal ratio method obtains the cross sections by measuring the ratio of reaction cross section between different de-excitation channels of the same compound nucleus. The external ratio method obtains the cross sections by measuring the ratio of reaction cross section of the same exit channel between different compound nuclei. Burke J T *et al.* [4] studied the $^{237}\text{U}(n, f)$ cross section by comparison with the well-measured $^{235}\text{U}(n, f)$ cross section. With $^{238}\text{U}(\alpha, \alpha' f)$ and $^{236}\text{U}(\alpha, \alpha' f)$ as the surrogate reactions, the cross section ratio between $^{237}\text{U}(n, f)$ and $^{235}\text{U}(n, f)$ was measured, then the $^{237}\text{U}(n, f)$ cross section was obtained by comparing with the perfect data of $^{235}\text{U}(n, f)$. This greatly reduces the systematic and theoretical calculation errors that exist in the direct surrogate reaction method [5].

1.3 Surrogate Capture Reaction Method

The existing SRM generally chooses the peripheral reactions of inelastic excitation or transfer reaction [1] as surrogate reaction, such as $(\alpha, \alpha' f)$ [6], (d, pf) [7], $(^3\text{He}, tf)$ [8], $(^{18}\text{O}, ^{16}\text{O}f)$ and so on. The angular momentum brought by peripheral reaction is generally dozens of \hbar . While the central reaction of the neutron capture reaction is in the low-angle momentum region, and the angular momentum of the compound nucleus is generally merely a few \hbar . As a result, the theoretical correction for the angular momentum, which is always essential for SRM, causes great difficulty in data analysis.

In view of this, we choose the capture reaction of light charged particle as the surrogate reaction, and use the compound nucleus as a bridge to obtain the neutron induced reaction cross sections, that is the surrogate capture reaction method (SCRM). As mentioned above, the angular momentum of the compound nucleus formed by light charged particle capture reaction is very low and close to that of the compound nucleus formed by neutron capture, therefore the deviation caused by the spin correction will be reduced. For example, to select $^{236}\text{U}(\alpha, 2n)$ as the surrogate reaction of $^{239}\text{Pu}(n, 2n)$ to generate the same compound nucleus ^{240}Pu , the average spins of the compound nucleus formed in $\alpha+^{236}\text{U}$ and $n+^{239}\text{Pu}$ were calculated

with PACE4 [9] and ECIS programs [10][11] respectively, as shown in Figure 2. It can be seen that the spin difference of the compound nucleus formed by the two pathways is small at the same excitation energy (E_x). The difference of the average spin $\Delta\langle J \rangle$ is also shown. In the excitation energy region of interest the spin difference is only $\pm 2 \hbar$ and little correction is expected (correction is ignored in the following analysis.).

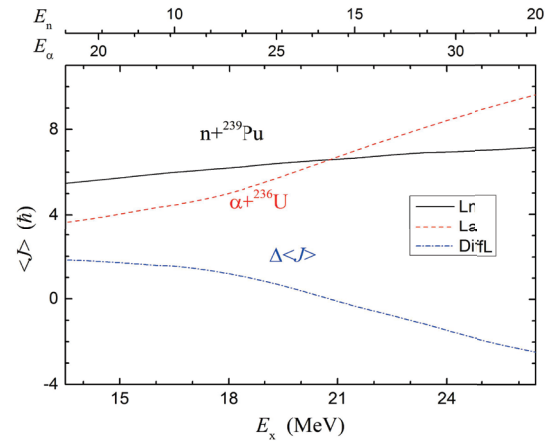


Figure 2. The average spins of the compound nucleus formed by neutron and α capture reactions and their difference.

Figure 3 shows the overall idea of the SCRM which takes $^{236}\text{U}(\alpha, 2n)$ as the surrogate reaction of $^{239}\text{Pu}(n, 2n)$. In the CN formation stage, the same CN excitation en-

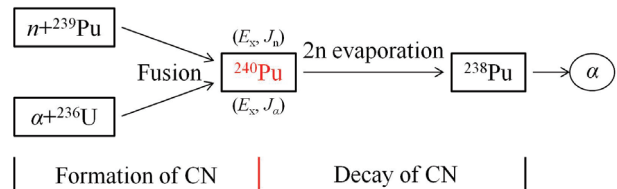


Figure 3. Schematic plot for the surrogate capture reaction method.

ergy by using $\alpha+^{236}\text{U}$ fusion as in neutron capture $n+^{239}\text{Pu}$ can be obtained by selecting the corresponding α energy, which is shown in Figure 2. In the decay stage ^{238}Pu is formed from the $2n$ evaporation channel. The $2n$ evaporation cross section of ^{240}Pu is obtained by measuring the α decay of ^{238}Pu , then the $^{239}\text{Pu}(n, 2n)$ cross section can be calculated:

$$\sigma_{(n,2n)} = \sigma_{(\alpha,2n)} \sigma_n^{cap} / \sigma_\alpha^{cap}, \quad (3)$$

σ_n^{cap} is the neutron capture cross section, which is basically a geometric cross section and changes slowly with energy and can be accurately calculated using the ECIS program [10][11], σ_α^{cap} is the fusion cross section for $\alpha + ^{236}\text{U}$ that can be accurately calculated using CC-FULL [12].

In addition, as the by-products of the $(n, 2n)$ cross section, (n, f) , $(n, 1n)$ and $(n, 3n)$ cross sections also can be extracted using SCRM. If the reaction cross section of a

certain reaction channel like (n, f) is already well measured, it can be used as a reference for further improving the data accuracy with the internal ratio method.

2 The application of SCRM - use $^{236}\text{U}(\alpha, 2n)$ as the surrogate reaction of $^{239}\text{Pu}(n, 2n)$

Based on the HI-13 tandem accelerator at the China Institute of Atomic Energy, $^{236}\text{U}(\alpha, 2n)$ were performed as the surrogate reaction of $^{239}\text{Pu}(n, 2n)$. The experiment can be divided into three steps:

1) The on-line experiment for measuring the angular distributions of elastic scattering and fusion-fission fragments of $\alpha+^{236}\text{U}$, then the optical potential and the fission excitation function can be obtained, which are helpful in constraining the α capture reaction cross section calculation and improving the accuracy;

2) The on-line irradiation of the ^{236}U targets, where 18 ^{236}U targets were irradiated with α beam at the same energies as in step 1;

3) Offline α radioactivity measurement, where α radioactivity of ^{238}Pu was measured to deduce the yield of $2n$ evaporation residual nucleus.

^{236}U target with a diameter of $\phi 5$ mm was electroplated onto $2\ \mu\text{m}$ thick aluminum foil. 2 thick targets of $5.0\ \mu\text{g}/\text{cm}^2$ were made for on-line experiment and 18 thin targets of $1.0\ \mu\text{g}/\text{cm}^2$ were made for on-line irradiation and off-line measurement.

2.1 The on-line experimental setup for $\alpha+^{236}\text{U}$

In the on-line experiment, eight $\phi 8$ mm Si(Au) detectors were used with a rotatable base for the angular distribution measurement of elastic scattering and fission fragments. At each energy point, the base plate was rotated in a step of 5° for three times, the elastic scattering and fission angular distribution can be obtained at totally 32 angles between $15^\circ \sim 162.8^\circ$. In addition, four Si(Au) detectors were placed symmetrically at the forward angle of 25° for monitoring the beam quality and cross section normalization. The α beam intensity was about $100 \sim 200$ enA.

2.2 The on-line irradiation of the ^{236}U targets

For the on-line irradiation, 18 uranium targets were divided into three groups for the higher, medium and lower energy α beams, corresponding α particle energies for all the 18 targets were $\{36.00, 32.01, 30.11, 28.12, 27.13, 26.12\}$, $\{26.11, 25.08, 24.02, 23.52, 23.03, 22.54\}$ and $\{22.55, 22.05, 21.05, 20.01, 18.98, 17.90\}$ MeV from higher to lower energies. Among them, there are two same energy points for connecting the different groups (the difference is within 10 keV), which can be used to check each other and help to obtain a smooth result.

The α beam intensity for the on-line irradiation was about $1.0\ \mu\text{A}$, and it was monitored by a water-cooling Faraday cup. In addition, a thin Au target (about $70\ \mu\text{g}/\text{cm}^2$) was placed behind the uranium targets for relatively normalizing the cross section and cross-check the beam energy at the last target.

2.3 The off-line measurement of α radioactivity

The radioactivity of the irradiated target samples were measured off-line. For the off-line measurement of α radioactivity, 18 target-detector measurement systems were manufactured. With the target-detector distance method, that is to measure the relationship between the counting rate and the target-detector distance, the absolute efficiency of each detector system can be calibrated to further improve the measurement accuracy.

In the off-line measurement, mainly the amount of ^{238}Pu generated through the $2n$ evaporation of CN was determined. ^{238}Pu has a half-life of 87.7 years and the decay α energies are 5.456 MeV (28.98 %) and 5.499 MeV (70.91 %), which are higher than the ^{236}U decay α energies of 4.445 MeV (26 %) and 4.494 MeV (74 %).

The off-line measurement energy spectra show two distinct peaks as shown in Fig. 4, corresponding to the α particles from ^{236}U and ^{238}Pu , respectively. The energy spectra prove that the purity of ^{236}U was extremely high and there's no interference from other radioactive impurity. The ratio of the two peak areas changes clearly with the α beam energy.

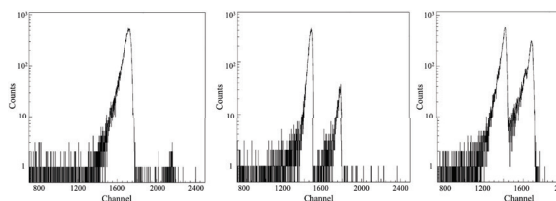


Figure 4. The off-line energy spectra of the irradiated ^{236}U targets, the α beam energies are 18.98, 21.06, and 32.01 MeV, respectively.

3 Data processing and analysis

3.1 Fission data analysis

Figure 5 shows the experimental results of the fission fragment angular distributions and the fitted results by using the saddle point transitional state theory [13] for the total 16 energy points between $17.93 \sim 36.00$ MeV. The fission excitation function can be obtained by integrating the angular distribution and then be used to verify the calculation result of CCFULL to improve the accuracy, since more than 90% CN de-excite by fission.

3.2 $\alpha+^{236}\text{U}$ data analysis

From the offline measured α radioactivity of ^{238}Pu , the total number of ^{238}Pu nuclei generated by $(\alpha, 2n)$ reaction can be obtained by using the exponential decay law for radioactivity. The number of ^{238}Pu can be taken as constant during the offline measurement considering the relatively long half-life. Combining the ^{236}U target thickness with the incident α particle number, the $2n$ evaporation cross section can be calculated:

$$\sigma(^4\text{He}, 2n) = \frac{N(^{238}\text{Pu})}{N(^{236}\text{U}) \cdot N(^4\text{He})}, \quad (4)$$

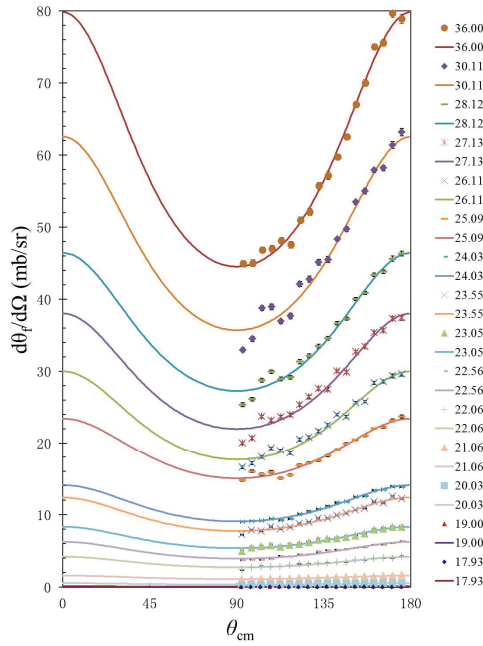


Figure 5. The angular distributions of fission fragments of the $\alpha+^{236}\text{U}$ reaction.

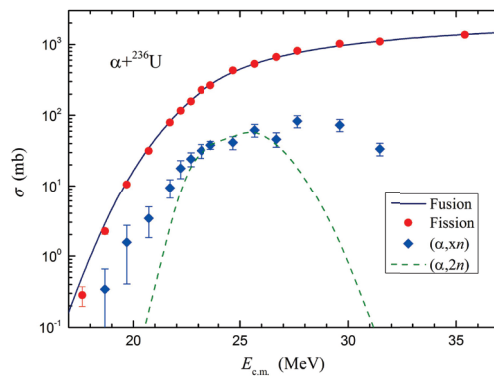


Figure 6. The fission and $2n$ evaporation excitation function for $\alpha+^{236}\text{U}$.

here $N(^{236}\text{U})$ is the number of ^{236}U nuclei per unit area and $N(^4\text{He})$ is the total number of the incident α particles.

Figure 6 shows the fission excitation functions and $2n$ evaporation channel of $\alpha+^{236}\text{U}$ system, the error bars are only the statistical errors. The dots represent the experimentally measured (α, f) cross sections, the solid line represents CCFULL calculation result for fusion, and the diamond points are the measured (α, xn) cross sections which contain $3n$ evaporation component at the higher energy region. It can be seen that the experimental measurement is in good agreement with the theoretical $(\alpha, 2n)$ cross sections of PACE4 [9] (dashed line) at the intermediated energy region of $E_\alpha = 22 \sim 27$ MeV.

3.3 Extraction of $^{239}\text{Pu}(n, f)$ and $^{239}\text{Pu}(n, 2n)$ cross sections with SCRM

Taking the compound nucleus ^{240}Pu as a bridge, the cross sections of $^{239}\text{Pu}(n, f)$ and $^{239}\text{Pu}(n, 2n)$ reactions can be

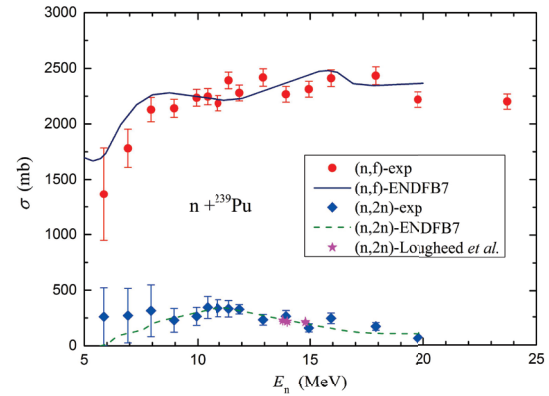


Figure 7. The $^{239}\text{Pu}(n, f)$ and $^{239}\text{Pu}(n, 2n)$ cross sections obtained by the present SCRM, the result by Lougheed R W *et al.* [17] and the evaluated nuclear data are also shown.

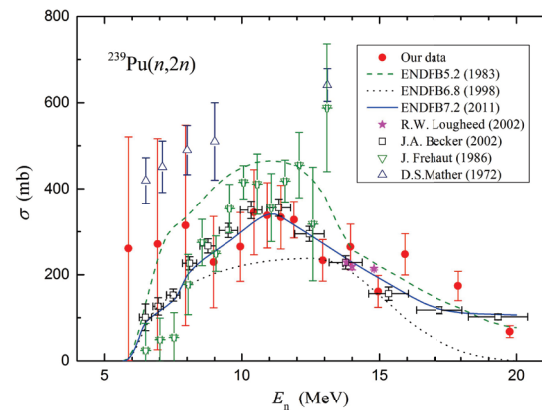


Figure 8. The $^{239}\text{Pu}(n, 2n)$ cross sections obtained by the present SCRM, and other experimental data [15][16][17][18] and ENDF data.

calculated with SCRM. The (n, f) (dots) and $(n, 2n)$ (diamonds) cross sections obtained with the present SCRM are shown in Figure 7. The data of ENDFB7 [14][15][16] is also plotted. It can be seen that the present results are consistent with both the evaluated nuclear data and the result by Lougheed R W *et al.* [17] within the error bars.

For $^{239}\text{Pu}(n, 2n)$, the evaluated nuclear data of ENDF differ greatly between the different versions. We chose the B5, B6, and B7 libraries and also the data of the related experiments $^{239}\text{Pu}(n, 2n)$ [15, 16] for comparison, as shown in Figure 8. Lougheed R W *et al.* [17] measured $^{239}\text{Pu}(n, 2n)$ with 14 MeV neutrons, and after more than 30 years tracking measurement of the α radioactivity of the residual nuclei, they obtained a more accurate $(n, 2n)$ cross section. It can be seen that our result is in good agreement with not only the data of B7 library, but also the more accurate $(n, 2n)$ cross section data around 14 MeV [17]. At the peak region of the $(n, 2n)$ cross section, i.e. E_n is about 11 ~ 12 MeV, the accuracy for the present data is better than 25%, at low energies ($E_n < 8$ MeV) the data accuracy becomes poor with the increasing statistical error.

4 Conclusion

The SCRM proposed here chooses the capture reaction of the light charged particles as the surrogate reaction for neutron capture. By employing the reaction cross section measurement of $^{236}\text{U}(\alpha, f)$ and $^{236}\text{U}(\alpha, 2n)$, the excitation functions of $^{239}\text{Pu}(n, f)$ and $^{239}\text{Pu}(n, 2n)$ reactions at $E_n = 5 \sim 20$ MeV energy region were obtained. The $^{239}\text{Pu}(n, f)$ and $(n, 2n)$ cross sections extracted indirectly by SCRM are consistent with that of ENDF within the error bars, demonstrating that SCRM is a powerful method for measuring the neutron reaction data of transuranium nuclei.

References

- [1] Escher J, Burke J T, Dietrich F S, *et al.* Rev. Mod. Phys., **84**, 353 (2012)
- [2] Cramer J D and Britt H C, Phys. Rev. C, **2**, 2350 (1970)
- [3] Plettner C, Ai H, Beausang C W, *et al.* Phys. Rev. C, **71**, 051602(R) (2005)
- [4] Burke J T, Bernstein L A, Escher J, *et al.* Phys. Rev. C, **73**, 054604 (2006)
- [5] Escher J and Dietrich F S, in Second Argonne/MSU/JINA/INTRIA Workshop, AIP Conf. Proc. **791**, 93 (2005)
- [6] Wang B S, Harke J T, Akindele O A, *et al.* Phys. Rev. C **100**, 064609 (2019)
- [7] Ducasse Q, Jurado B, Aiche M, *et al.* Phys. Rev. C. **94**, 024614 (2016)
- [8] Basunia M S, Clark R M, Bernstein L A, *et al.* AIP Conf. Proc. **1005**, 101 (2008)
- [9] fusion-evaporation code, <http://lise.nsl.msue.edu/lise.html>
- [10] Raynal J, Technical Report No. SMR-9/8, IAEA
- [11] Raynal J, ICTP International Seminar Course (IAEA, ICTP, Trieste, Italy, 1972 p. 281)
- [12] Hagino K, Rowley N, Kruppa A T, Comput. Phys. Communi., **123**, 143-152 (1999)
- [13] Bohr A, Proc. 1st Int. Conf. Peaceful Uses Atomic Energy (United Nations, New York), **2**, 151 (1956)
- [14] Carlson A D, Pronyaev V, Hale G H, *et al.*, EPJ Web of Conferences, **146**, 02025 (2017)
- [15] Bernstein L A, Becker J A, Garrett P E, *et al.*, Phys. Rev. C, **65**, 021601(R) (2002)
- [16] Frehaut J, *et al.* Nucl. Sci. Eng., **74**, 29 (1980)
- [17] Loughheed R W, Webster W, Namboodiri M N, *et al.*, Radiochim. Acta, **90**, 833 (2002)
- [18] Mather D S, Bampton P F, Coles R E, *et al.*, Nind, P. J.: Report AWRE-O-72/72 (1972), Report AWRE-O-47/, 69 (1969)